Monte Carlo simulation of pulsed laser ablation from two-component target into diluted ambient gas

T. E. Itina[a)]
Laboratoire Interdisciplinaire Ablation Laser et Applications, IRPHE-LP3 UMR CNRS 6594, Parc Scientifique et Technologique de Luminy, 163 avenue de Luminy, Case 918, Marseille 13009, France

W. Marine
Laboratoire Interdisciplinaire Ablation Laser et Applications, GPEC UMR CNRS 6631, Parc Scientifique et Technologique de Luminy, 163 avenue de Luminy, Case 918, Marseille 13009, France

M. Autric
Laboratoire Interdisciplinaire Ablation Laser et Applications, IRPHE-LP3 UMR CNRS 6594, Parc Scientifique et Technologique de Luminy, 163 avenue de Luminy, Case 918, Marseille 13009, France

(Received 25 March 1997; accepted for publication 30 May 1997)

Laser ablation from a binary target into a diluted gas background is studied by means of a Monte Carlo simulation. The influence of the ambient gas on the spatial and mean energy distribution of particles deposited at the distant detector is considered. Thermalization of the particles, the random scattering effect and the backscattering of particles were observed. Considerable modification of the deposited film thickness profiles due to collisions of the ablated particles with the ambient gas is shown. The increase of the ambient gas pressure was found to affect the stoichiometry distribution of deposited and backscattered particles. The study is of a particular interest for the development of the thin film growing technique known as pulsed laser deposition. © *1997 American Institute of Physics.* [S0021-8979(97)04617-3]

I. INTRODUCTION

Pulsed laser deposition (PLD)[1,2] for growing thin films is one laser application that has progressed rapidly over past few years. Interest in this field was brought about by the success of *in situ* growth of high-temperature superconducting films.[3] Numerous experiments were carried out and rich scientific information of the ablation process was obtained. Of particular interest was the influence of various laser parameters, system geometry, target material and ambient gas on the film thickness profile and film stoichiometry. Experimental and theoretical studies[4–17] show the formation of a forward-peaked angular distribution of the ablated particles. In vacuum, collisions of the plume particles among themselves were found[9–17] to determine the plume angular distribution. The effects of the background gas on the deposition process were considered in a number of papers. The experimental results on ablation in the presence of ambient gas[8,18–20] revealed the dependence of the deposition rate on the ambient gas parameters. The comparison between the results obtained for the deposition in inert and reactive atmospheres ensured that part of these effects is not chemical in nature.[8]

In the presence of ambient gas, additional plume particle collisions with the background gas must be considered.[21] Previous investigations show that the effect of background gas depends on the pressure regime and on the laser parameters used in PLD. For an accurate description of this effect one must distinguish between two cases. In the first case the density of the ablated particles is so high that the plume can be described in terms of a continues medium. As a rule, the ambient gas pressures of a few hundreds of mTorr are used in these experiments. For this regime shock wave models[22–24] are found to describe the interaction well. Fast photographic techniques were used to study the process and forward focusing of the plume was often observed. When the density and the energy of the ablated particles are not very high, plume-background gas interaction can be considered as the scattering of a molecular beam by the particles of the background gas. For very low ambient gas pressure ($P \leqslant 0.66$ Pa), attenuation of a molecular beam by elastic collisions was observed.[25] The higher gas pressure (up to 200 mTorr $= 26.4$ Pa) regime is of a particular interest because it is frequently used in PLD. Under these conditions, the influence of the ambient gas on the film thickness profile has not been theoretically investigated sufficiently and these effects are not yet clear. For instance, several papers report broadening of the angular distribution of the ablated particles as a result of scattering processes in the background gas,[8,19,26–28] while the focusing effect was observed by other authors.[21,29,30] The increase of the backscattering of particles is also an important effect of ambient gas that can influence the deposition process. In fact, collisions of the ablated particles with the background gas result in a decrease of the number of the ablated particles arriving at the substrate. If the pressure of the ambient gas is sufficiently high, the backscattered flow can even exceed the flow of particles reaching the substrate. This process significantly influences the composition of the deposited material and the state of the irradiated surface. The uniformity of the film stoichiometry, which is critical for a number of materials, can be also affected by the ambient gas.

To investigate these phenomena we carried out a three-dimensional Monte Carlo[31] (MC) simulation. We considered the laser ablation from a binary target into a diluted ambient

[a)]On leave from The Moscow Institute of Physics and Technology, Russia. Electronic mail: michel.autric@irphe-lp3.univ_mrs.fr

 © 1997 American Institute of Physics

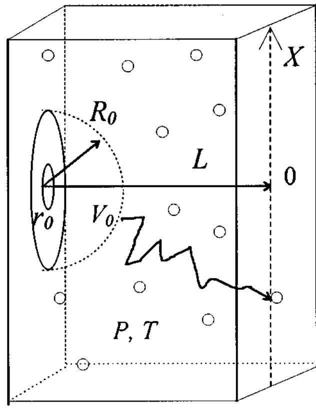

FIG. 1. Illustration of the geometry problem. Inside V_0 the flow is modeled using the DSMC method; outside V_0 the random trajectories in the ambient gas are simulated by the RTMC algorithm.

gas (pressure up to 100 mTorr) when the desorption flux is not very high (a few monolayers per laser pulse). We used a three-dimensional algorithm that combines both the direct simulation Monte Carlo (DSMC) technique[11–17,32] (to simulate the formation of the gas cloud and its initial expansion) and the Monte Carlo simulation of the random trajectories (MCRT) of the ablated particles in the ambient gas.[21,33,34] This approach allowed us to simulate both the collisions among the ablated particles and interactions of the ablated particles with the background gas particles. The influence of these collisions on the spatial distribution of film thickness, mean energy and stoichiometrical ratio of the particles deposited at the distant substrate and scattered back to the irradiated surface was considered.

II. SIMULATION

A. Combined "direct simulation-random trajectories simulation" Monte Carlo method

We assume that the process of laser ablation in the diluted ambient gas consists of two parts:

(i) desorption and initial expansion when collisions of the ablated particles among themselves are significant and the influence of the ambient gas can be disregarded;

(ii) the expansion of the gas cloud in the ambient gas when collisions of the ablated particles among themselves can be disregarded.

Based on these assumptions, we performed the Monte Carlo simulation using two different techniques. The desorption and initial expansion were modeled by a DSMC algorithm. In this method, the motion of a number of test particles is simulated and the gas flow evolves in time. Simulation of the initial stage of the process is performed in the finite volume V_0 of the physical space (see Fig.1). The calculations start when the volume is empty and the particles desorb from the surface. Above the surface the particles can collide, and a gas cloud moves away from the surface. At the border of the volume V_0 we set the following boundary conditions: the backscattered particles are assumed to recondense on the irradiated surface, and the motion of each of the particles leaving V_0 in the outward direction is simulated like a random trajectory in the ambient gas using the MCRT algorithm described below. The trajectory is modeled independently until the particle reaches the distant substrate or until it is redeposited on the irradiated surface. In the present modeling, we neglected the difference in the sticking probability for species with different masses and assumed the unit incorporation probability at the substrate and at the target (for backscattered particles) for both species.

It should be noted that the approach described above is justified if

(i) the mean free path in the background gas is longer than a cloud dimension at the end of the first expansion process;

(ii) beyond the volume V_0 collisions of the ablated particles among themselves can be disregarded.

It can be shown[21] that for typical ablation experiments these assumptions are valid if the linear dimensions of V_0 are in the range $L_0 \leqslant R_0 \leqslant \lambda_f$, where L_0 is the distance beyond which collisions among the ablated particles can be disregarded and λ_f is the mean free path of the ablated particles in the ambient gas. Taking the temperature of the ambient gas to be $T=300$ K and $R_0 \sim 1.5$ mm yields the upper limit for a background pressure of about 100 Pa = 760 mTorr.

B. Initial expansion (DSMC method)

We suppose that particles desorb from a circular area (πr_0^2) of a plane target during a laser pulse time τ. The target material is composed of two species with the masses m_1 and m_2 ($m_1 < m_2$). The initial velocity distribution is the Maxwell-Bolzmann distribution with the same temperature T_0 for both species. The collisions between the ablated particles (a-a collisions) are simulated using hard-sphere collision dynamics with the identical (for simplicity) collision cross sections $\Sigma_{\rm aa}$ for both species. We assume that the number of monolayers desorbed during one laser pulse is

$$\theta = \Phi \cdot \Sigma_s \cdot \tau, \tag{1}$$

where $\Sigma_s = \Sigma_{aa}/4$ is the area atom occupies at the surface, $\Phi = (n_1 V_1 + n_2 V_2)/2$ is the total desorption flux, V_i is the thermal velocity of the component i, and n_i is the density of the desorbed gas immediately in front of the surface (we assume $n_1 = n_2$). The factor of 2 is included in the denominator of the expression for Φ since the desorbed current has a cosine distribution. To determine the radius of the evaporated area we use the parameter

$$b = \frac{r_0}{V_1 \tau}, \tag{2}$$

where $V_1 \tau$ is the length of the light particle cloud at the end of the laser pulse.

For calculation of the formation and initial expansion of the ablated plume we used the DSMC method based on Bird's algorithm.[32] We set $b=5$ and $\theta = 3$ in all the calculations presented here. It can be shown[16,17] that for these parameters collisions among the ablated particles can be dis-

regarded beyond the distance $L_0 \sim 50\ V_1\tau$. Taking $V_T = 10^3$ m/s and $\tau = 3\times10^{-8}$ gives $L_0 \sim 1.5$ mm. The simulation was performed in the hemispherical volume with the radius $R_0 = 50\ V_1\tau$ and cylindrical symmetry was assumed. Bird's algorithm was improved by the last-collision technique proposed by NoorBatcha *et al.*[11] The computer's code was tested by comparing the results of the version for the ablation in vacuum with the results of similar calculations by Urbassek and Sibold.[16] Setting $\theta = 3.6$, $b=5$, $m_1:m_2= 1:5$ and the ambient gas pressure $P = 0.01$ mTorr, a very reasonable agreement with the results of Ref. 16 was obtained. The angular characteristics of the flow were reproduced to within 5% (we do not present these curves here).

C. Expansion in the ambient gas (MCRT method)

As soon as a particle leaves the volume V_0 its motion is simulated as a random trajectory in the ambient gas (mass m_3). The collisions between the ablated particles and the background gas particles are assumed to be a random process described by a Poisson distribution. A free flight path λ between two collisions of the ablated particle with the background particles (a-b collisions) is simulated as

$$\lambda = -\Lambda \cdot \ln(R_1), \tag{3}$$

where R_1 is a random number uniformly distribute between 0 and 1, and Λ is assumed to be

$$\Lambda = \frac{1}{P\Sigma_{ab}}\sqrt{\frac{EkT}{2\pi}}. \tag{4}$$

Here E is the kinetic energy of the ablated particle before the collision, T is the temperature of the ambient gas, k is Bolzmann's constant, P is the pressure of the ambient gas, and Σ_{ab} is the ablated particle-background particle collision cross section. The a-b collisions are also calculated using the model of hard spheres. The background particles are supposed to be at rest in the laboratory reference frame before the collision. The post-collision motion of the background gas is ignored. If the energy of the ablated particle drops below the mean energy of the background particles E_{amb} at temperature T, the particle is supposed to be *thermalized*[34] and its energy is no longer modified. The trajectory of each particle is simulated until it crosses the plane parallel to the target at a distance L or it is redeposited on the target.

We note that the assumption that the background particle is at rest before the collision results in an error in energy transfer of the order of E_{amb}. The motion of the background gas can be ignored if the gas pressure is not high (below 200 mTorr). In other cases the sufficient fraction of the background particles undergoes collisions[21] that result in the collective motion of the background gas toward the substrate and even in the traveling of shock waves[22–24] in front of the ablation plume.

III. RESULTS AND DISCUSSION

We present the results of simulation with the parameters that are typical for pulsed laser desorption for laser fluences close to the ablation threshold. We set $\tau = 3\times10^{-8}$ sec, and $T_0 = 2901.25$ K. The masses of the ablated particles were assumed to be in the ratio of $m_2:m_1 = 2:1$, where $m_1 = 63.54$ amu (Cu atoms). The ambient gas was supposed to be Ar ($m_3:m_1 = 0.63$) with the temperature $T = 273$ K. For simplicity, we used the identical cross section $\Sigma_{ab} = 25.1$ Å^2 of a collision with the particle of the ambient gas for both species. We set the target-substrate distance to $L = 5$ cm in all the calculations. The ambient gas pressure P was varied in the range 0.01 mTorr (''vacuum'')–100 mTorr. We note that the results will be the same within statistical fluctuations when the product $P\times L$ of the filling gas pressure and the target-substrate separation is kept constant.[30,35] Thus, results for other values of L can be found by rescaling the ambient gas pressure. We used the total number of 10^6 particles and repeated it five times to gain enough statistics. For all the simulation results, the 95% confidence error bars are smaller than the size of the symbols.

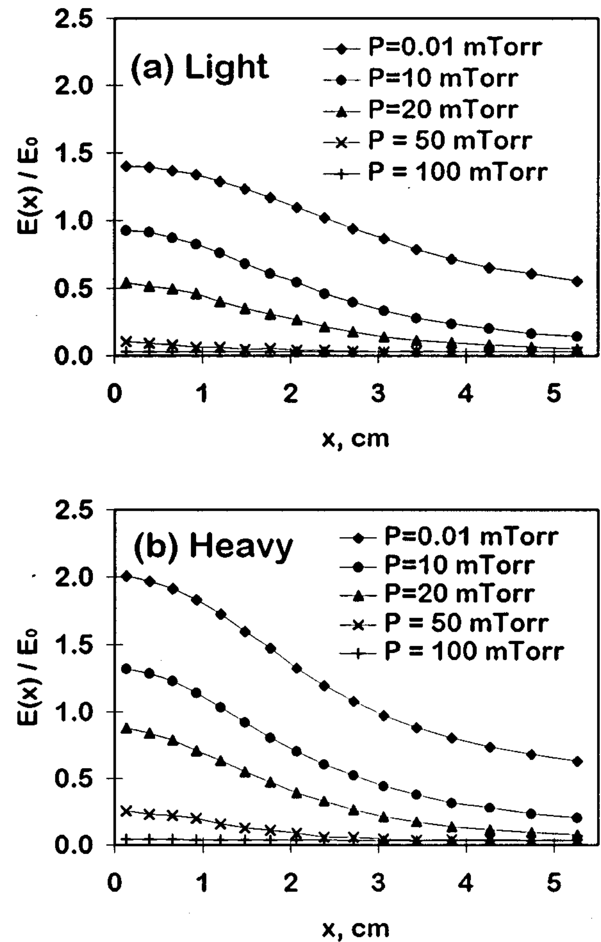

FIG. 2. Mean energy $E(x)$ of light (a) and heavy (b) particles deposited at a plane substrate as a function of radial distance from the center of the substrate. The distributions were normalized by $E_0 = 2kT_0$, where T_0 is the temperature of the surface.

Fig. 2 shows the distribution of the mean kinetic energy $E(x)$ of particles deposited at the plane substrate as a function of the radial distance from the center of the substrate. We note that in vacuum ($P = 0.01$ mTorr) heavy particles are more energetic than light particles and their distribution of mean energy is more focused toward the center. With an increase of the background pressure the mean energies of

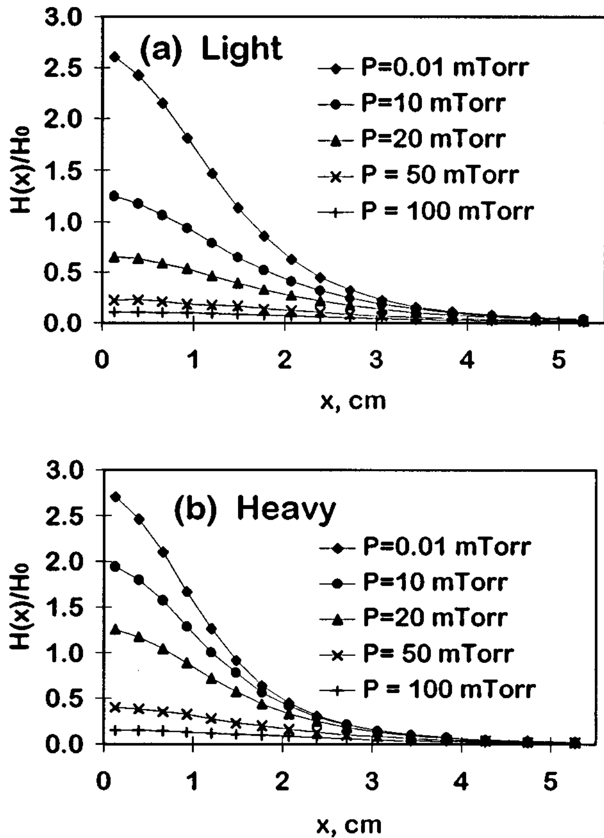

FIG. 3. Spatial distributions $H(x)$ of the number of particles deposited per unit area at the plane substrate, where x is a radial distance from the center of the substrate. The distribution of (a) light particles for different values of the ambient gas pressure; (b) the same for heavy particles. All distributions were normalized by $H_0=N_{tot}/(\pi L^2)$, were N_{tot} is the total number of the ablated particles and L is the target-substrate distance.

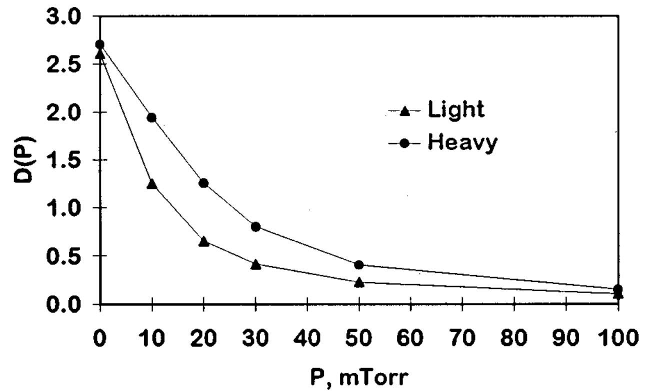

FIG. 4. The deposition rate $D(P)$ of heavy and light particles as a function of the ambient gas pressure. It was calculated as the number of particles $H(x = 0)$ deposited at the center of the plane substrate per one laser pulse per unit area. The distributions were normalized by $H_0=N_{tot}/(\pi L^2)$, where N_{tot} is the total number of the ablated particles and L is the target-substrate distance.

both species diminish and the distributions become less focused toward the center. This effect is more pronounced for light particles than for heavy particles.

Fig. 3 displays the deposition profiles $H(x)$ of particles arriving at the plane substrate. These profiles represent the relative number of particles deposited per unit area as a function of the radial distance from the center of the substrate. All the curves were normalized by the same value and can be compared. The deposition profiles of light species for different values of the ambient gas pressure are shown in Fig. 3(a), and the profiles of heavy particles for the same values of the background gas pressure are displayed in Fig. 3(b). It can be observed that the number of both species reaching the substrate decreases with the increase of pressure. Moreover, the distributions of both species become less peaked as the pressure increases. These effects are more pronounced for light species than for heavy ones.

The decrease of the kinetic energy of the ablated particles can be explained by the energy lost in collisions with the background gas. Due to these collisions, the part of the particles reaching the substrate is thermalized. When the pressure increases, the fraction of the thermalized particles increases. The decline of energy is more pronounced for light particles since they loose energy more efficiently in a collision. Thus, a smaller background pressure is required for thermalization of light components. Since the trajectories of thermalized particles can be considered as a random walk in ambient gas, after a sufficient number of collisions the particles are scattered randomly from their initial trajectories. The random scattering results in the dispersion of the angular distribution of the mean energy. When the pressure is sufficiently high ($P\sim 100$ mTorr) most of both species are thermalized and both mean energy distributions become almost uniform. Collisions of the plume particles with the particles of the background gas perturb the initial angular distributions that were formed after the first stage of the expansion process. As a result of the random scattering processes, the angular distributions of particles become broadened from the surface normal. Moreover, a substantial fraction of particles is scattered back and is recondensed on the irradiated surface. The backscattering process results in a decrease of the number of the particles arriving at the substrate and the deposition profiles become thinner. We note that the broadening effects induced by collisions might be expected to begin appearing when the mean free path of an ablated particle in the filling gas starts to become less than the target-substrate distance.[29] Taking the mean free path $\lambda_0 \sim(\sqrt{2}\cdot n\Sigma_{ab})^{-1}$ and $L=5$ cm gives the pressure $P\sim 2$ mTorr required for the appearance of the dispersive effect of collisions. At higher ambient gas pressures the condition $\lambda_0/L<1$ is well fulfilled (for example at $P=100$ mTorr we have $\lambda_0/L\sim 0.02$). Thus, under the conditions used in present modeling, the propagation of the ablated plume into a diluted gas can be considered as a diffusion-like process. Hence, one can expect the density of the ablated flux to diminish exponentially as a function of distance and the amount of material reaching the substrate to decrease when pressure is increased.

Fig. 4 shows the effect of the increase in the background gas pressure on the deposition rate $D(P)$ for both species. One can see that the deposition rate decreases with the pressure. At low pressures the deposition rate of light particles decreases more rapidly than that of heavy particles, whereas

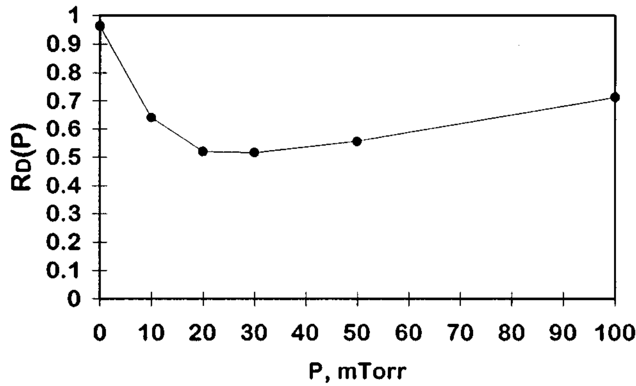

FIG. 5. The ratio $R_D(P)$ of the deposition rate of light species to that of heavy species as a function of the ambient gas pressure. Here, R_D represents the ratio of the number of light species deposited at the center of the plane substrate per unit area to that of heavy species.

at higher pressures the decline is more rapid for heavy particles. In addition, one can see that the difference between $D(P)$ for light and heavy particles increases at low pressures ($P<20$ mTorr) and diminishes at higher pressures (20 mTorr $<P<100$ mTorr). These effects can be clearly observed in Fig. 5 that illustrates the ratio $R_D(P)$ of the deposition rate of light species to the one of heavy species as a function of background gas pressure. These results can be explained by the difference between the gas pressures required for thermalization of heavy and light particles. It is obvious that the thermalization of light particles occurs at lower pressure. Thus, there is a pressure range when most of the light particles are already thermalized but the thermalization of heavy species continues.

The distributions of the stoichiometrical ratio $R_S(x)$ of the particles deposited at a plane substrate for different values of background pressure are shown in Fig. 6. In this case, $R_S(x)$ represents the ratio of the number of light species deposited per unit substrate area to one of heavy species,

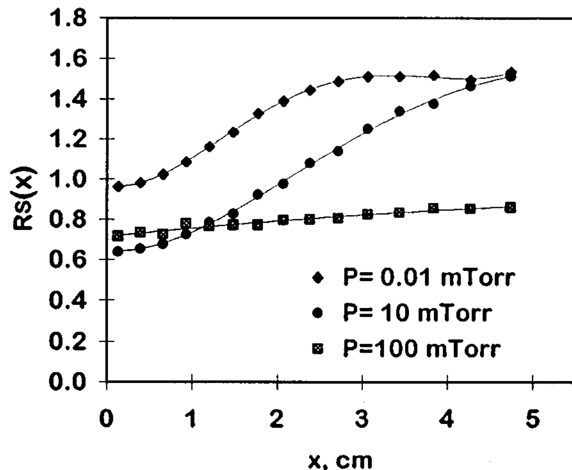

FIG. 6. The spatial distribution of the ratio $R_S(x)$ of the number of light particles deposited at the plane substrate to that of heavy particles. Here x is a radial distance from the center of the substrate.

where x is the radial distance from the center of the substrate. One can see that at low ambient gas pressure the ratio $R_S(x)$ is higher than the one at higher P. The lack of light particles at distances close to the substrate center can be also observed at low background gas pressures. With an increase of pressure it becomes smaller and when the gas pressure is sufficiently high ($P=100$ mTorr) the distribution $R_S(x)$ becomes almost uniform along the substrate.

The lack of light species at distances close to the substrate center at low background gas pressures can be explained by the fact that the angular distribution of heavy species formed after the initial expansion process is more focused toward the surface normal.[16] This result can be understood if one consider collision kinematics. In a binary gas mixture, light particles have a higher probability for large-angle scattering. In addition, heavy particles are accelerated by light ones. This process takes place as long as there is a region in the flow where both species are mixed. In the present simulation this region is present in the back of the gas cloud. The total number of light species arriving at the substrate in vacuum is higher than the one of heavy species due to the assumption $n_1=n_2$ that fixes the desorption fluxes $\Phi_1:\Phi_2=\sqrt{2}:1$. The collisions with the background gas result in the decrease of the number of deposited particles. The effect is more pronounced for light particles. As a result of the more intense backscattering of light particles, the stoichiometrical ratio $R_S(x)$ decreases. Since the deposition profiles of light and heavy particles both become more uniform with the increase of pressure, the distribution of the stoichiometrical ratio becomes more uniform when increasing the gas pressure.

As we already noted, due to both a-a and a-b collisions the ablated particles can be scattered back toward the irradiated surface. The spatial distributions $H_S(x)$ of the backscattered particles are presented in Fig. 7, where x is the radial distance from the center of the evaporated area. One can see that collisions with the ambient gas lead to a significant increase in the number of particles scattered back. This increase is more pronounced for light particles [Fig. 7(a)] than for heavy particles [Fig. 7(b)]. The peaks of both distributions at distances close to the center of the laser spot can be attributed to the particles scattered back as a result of collisions of the ablated particles among themselves at the initial stage of the process. Since these particles were recondensed on the small area (about the area of the laser spot), the number of particles per unit area is high. Collisions of the ablated particles with the background gas particles, on the other hand, lead to recondensation at the large area. The number of particles recondensed per unit area as a result of these processes is smaller than the one as a result of collisions inside the ablated gas cloud. One can also observe that the number of light particles scattered back as a result of collisions is higher than the number of heavy particles. We note from the Fig. 7 that at pressure $P=100$ mTorr both distributions are almost uniform for $x>r_0$. This result can again be attributed to the gas scattering processes that disperse the initial trajectories of the ablated particles and force the particles to be distributed in space more uniformly.

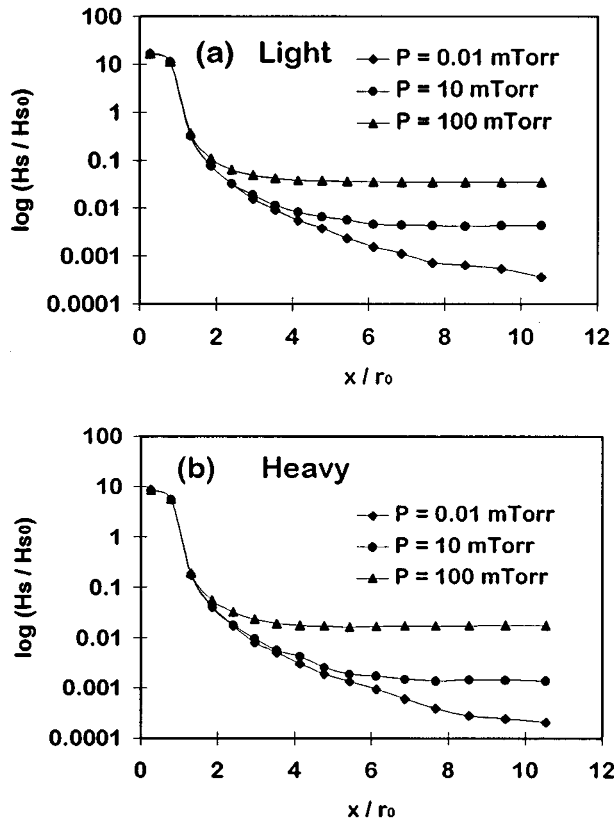

FIG. 7. Spatial distributions $H_S(x)$ of the number of particles scattered back and recondensed (per unit area) at the irradiated surface. Here x is a radial distance from the center of the evaporated area. The distributions of (a) light species for different values of the ambient gas pressure; (b) the same for heavy species. All distributions were normalized by $H_{s0}=N_{tot}/(\pi R_0^2)$, where N_{tot} is the total number of ablated particles and $R_0=50V_T\tau$, V_T is a thermal velocity at the temperature of the surface, and τ is the time of desorption.

The distributions of the stoichiometrical ratio $R_S(x)$ of the particles scattered back at the surface are shown in Fig. 8. In this case, $R_S(x)$ represents the ratio of the number of the light species deposited per unit surface area to the one of heavy species, where x is the radial distance from the center of the evaporated area. One can see that at low ambient gas pressure the distribution is not uniform; it has a minimum at $x \sim 2r_0$ and a maximum at $x \sim 8r_0$. Furthermore, one can see that at $P=100$ mTorr the stoichiometrical ratio of the backscattered particles is almost uniformly distributed along the surface. This result can be explained by the increase of the uniformity of the distributions of both backscattered species at high pressure.

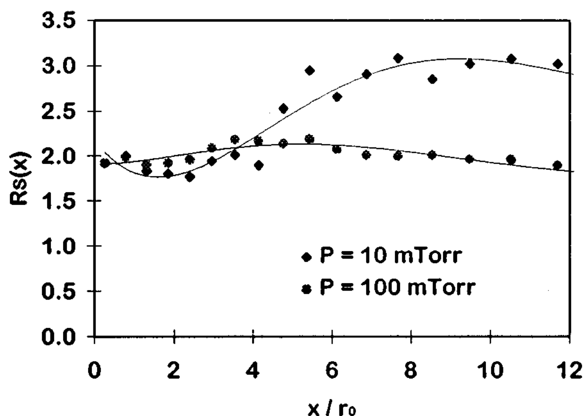

FIG. 8. The ratio $R_S(x)$ of the number of light species recondensed on the irradiated surface to that of heavy species as a function of radial distance from the center of the irradiated area.

The results obtained in the present study are in agreement with several experimental findings,[8,19,26–28] where the broadening of the angular distributions and the decrease of the deposition rate due to the scattering processes in the ambient gas were observed. For example, Lichtenwalner *et al.*[8] investigated the ablated flux characteristics of PZT, LCS and MgO ceramic targets as a function of chamber pressure for different gases (O_2 and noble gases). They found that, at low laser power, the deposition rate decreases and the plume broadens as the gas pressure is increased. Narrowing of the ablation plume was also observed by these authors, but at high laser energies and high gas pressures. We note that the focusing effect was found to occur when the ablated flux density and the background gas density are near the viscous flow level. Leuchtner *et al.*[29] investigated deposition of platinum films in an oxygen atmosphere. They also revealed different pressure regimes. In particular, the deposition rate was found to decrease as the O_2 pressure was increased from 50 mTorr to 300 mTorr. This result was attributed to the scattering of platinum atoms in the background gas. An increase in film uniformity when increasing the background pressure was also experimentally observed. For example, Rouleau *et al.*[20] performed growth of highly doped p-ZnTe(100) GaAs epilayers by pulsed laser ablation of a stoichiometric ZnTe target through N_2 ambient gas. They showed an increase of the uniformity of film stoichiometry when the background gas pressure is as high as $P=100$ mTorr. We note that this result is in a reasonable agreement with the results of our simulation. In addition, the possibility of the deposition of the compositionally uniform YBaCuO films at the appropriate values of background pressure and target-substrate distance was shown by Foote *et al.*[28] This result was attributed to the species-dependent gas scattering processes that compensated the vacuum composition nonuniformities.

IV. CONCLUSIONS

The process of laser ablation from the two-component target into the diluted background gas ($P \leqslant 100$ mTorr) was studied by Monte Carlo simulation. The approach developed in this article has allowed us to consider both the interactions between ablated particles and ablated particles-background gas atoms collisions. The latter were found to decrease the kinetic energy of particles. We have observed that at sufficiently high background pressure both species become thermalized. The thermalized particles are randomly scattered from their initial trajectories that results in more uniform angular characteristics of the flow. This thermalization phenomenon appears at different pressures for light and heavy particles. Our results show that an ambient gas pressure about 50 mTorr is required for thermalization of most of the

light species while a somewhat higher pressure ($P \sim 100$ mTorr) is necessary to thermalize most of the high particles. There is, therefore, a pressure regime where most of the light particles are thermalized, while a fraction of heavy particles retains its energy. At background gas pressures $P > 100$ mTorr most of both species were found to reach the substrate thermalized.

The collisions of ablated particles with ambient gas were shown to disturb the angular distribution of particles formed as a result of the initial expansion process. The deposition profiles of both species were found to become broadened as a result of collisions with background gas particles. Furthermore, the film thicknesses of both deposited components were shown to decrease with an increase of background pressure. The deposition rate decline was connected with the thermalization process. Due to the difference between the pressures required for thermalization of particles with different masses, the deposition rate of light particles diminishes significantly at smaller ambient gas pressures than those of heavy particles. The background gas was found to influence the stoichiometrical ratio of species with different masses. We have ascertained that the increase of gas pressure results in extension of the uniformity of the stoichiometry distribution along the substrate. Our results show that compositionally uniform films can be obtained at the appropriate background gas pressure when the intrinsic composition nonuniformities are concealed due to species-dependent gas scattering effects.

In addition, we have shown that the particles scattered back as a result of collisions between the ablated particles among themselves are recondensed on the surface area at about the area of the laser spot, whereas the particles scattered back as a result of collisions with the ambient gas are recondensed on the larger area. The increase of the background pressure was found to give rise to the more uniform distribution of the recondensed particles and of the stoichiometrical ratio along the surface.

The results obtained are of a particular interest for an understanding of the laser ablation process in ambient gas. They can be useful for developing pulsed laser deposition technology for materials with strict stoichiometry requirements.

ACKNOWLEDGMENT

One of the authors (T.E.I) gratefully acknowledges the Ministère des Affaires Etrangères, France, for financial support.

[1] *Laser Ablation for Materials Synthesis*, edited by D.C. Paine and J.C. Brauman, (MRS, Pittsburg, PA, 1990).
[2] *Pulsed Laser Deposition of Thin Films*, edited by D.B. Chrisey and C.K. Hubler (Naval Research Laboratory, Washington, DC, 1994).
[3] D. Dijkkamp, T. Venkatesan, X. D. Wu, S. A. Shaheen, N. Jisrawi, Y. H. Min-Lee, W. L. McLean, and M. Croft, Appl. Phys. Lett. **51**, 619 (1987).
[4] T. Venkatesan, X. D. Wu, A. Inam, and J. B. Wachtman, Appl. Phys. Lett. **52**, 1193 (1988).
[5] R. Foltyn, R. E. Meunchausen, R. C. Dye, X. D. Wu, L. Luo, D. W. Cooke, and R. C. Taber, Appl. Phys. Lett. **59**, 1374 (1991).
[6] A. Namiki, T. Kawai, and K. Ichige, Surf. Sci. **166**, 562 (1986).
[7] A. Namiki, K. Katoh, Y. Yamashita, Y. Matsumoto, H. Amano, and I. Akasaki, J. Appl. Phys. **70**, 3268 (1991).
[8] D. J. Lichtenwalner, O. Auciello, R. Dat, and A. I. Kingon, J. Appl. Phys. **74**, 7497 (1993).
[9] J. P. Cowin, D. J. Auerbach, C. Becker, and L. Wharton, Surf. Sci. **78**, 545 (1978); **84**, 641(E) (1979).
[10] R. Kelly and R. W. Dreyfus, Nucl. Instrum. Methods Phys. Res. B **32**, 314 (1988).
[11] I. NoorBatcha, R. R. Lucchese, and Y. Zeiri, J. Chem. Phys. **86**, 5816 (1987).
[12] I. NoorBatcha, R. R. Lucchese, and Y. Zeiri, Phys. Rev. B **36**, 4978 (1987).
[13] I. NoorBatcha, R. R. Lucchese, and Y. Zeiri, J. Chem. Phys. **89**, 5251 (1988).
[14] I. NoorBatcha, R. R. Lucchese, and Y. Zeiri, Surf. Sci. **200**, 113 (1988).
[15] D. Sibold and H. M. Urbassek, Phys. Rev. A **43**, 6722 (1991).
[16] H. M. Urbassek and D. Sibold, Phys. Rev. Lett. **70**, 1886 (1993).
[17] D. Sibold and H. M. Urbassek, J. Appl. Phys. **73**, 8544 (1993).
[18] D. B. Geohegan, Appl. Phys. Lett. **60**, 2732 (1992).
[19] J. Gonzalo, C. N. Afonso, J. Perrière, R. Gomez, and San Roman, Appl. Surf. Sci. **96-98**, 693 (1996).
[20] C. M. Rouleau, D. H. Lowndes, J. W. McCamy, J. D. Budai, D. B. Poker, D. B. Geohegan, A. A. Puretzky, and S. Zhy, Appl. Phys. Lett. **67**, 2545 (1995).
[21] J. C. S. Kools, J. Appl. Phys. **74**, 6401 (1993).
[22] P. E. Dyer, A. Isaa, and P. H. Key, Appl. Phys. Lett. **57**, 186 (1990).
[23] R. Kelly, A. Miotello, B. Braren, A. Gupta, and K. Casey, Nucl. Instrum. Methods Phys. Res. B **65**, 187 (1992).
[24] A. Gupta, B. Braren, K. G. Casey, B. W. Hussey, and R. Kelly, Appl. Phys. Lett. **59**, 1302 (1991).
[25] R. E. Leuchtner, J. S. Horwitz, and D. B. Chrisey, presented at the Materials Research Society Fall Meeting, Boston, MA, 1991 (unpublished).
[26] See, for example, K. L. Saenger, Summary of Angular Distribution Results for PLD in Gas Ambient, in Ref. 2, Chap. 7, p. 206.
[27] A. A. Gorbunov and V. I. Konov, Sov. Phys. Tech. Phys. **34**, 77 (1989).
[28] M. C. Foote, D. B. Jones, D. B. Hunt, J. B. Barner, R. P. Vasquez, and L. J. Bajuk, Physica C **201**, 176 (1992).
[29] R. E. Leuchtner, D. B. Chrisey, and K. S. Grabowski, Surf. Coat. Technol. **51**, 476 (1992).
[30] G. M. Turner, I. S. Falconer, B. W. Jamesand, and D. R. McKenzie, J. Vac. Sci. Technol. A **10**, 455 (1992).
[31] M. H. Kalos and P. A. Whitlock, *Monte Carlo Methods* (Wiley, New York, 1986).
[32] G. A. Bird, *Molecular Gas Dynamics* (Clarendon, Oxford, 1976).
[33] R. E. Somekh, J. Vac. Sci. Technol. A **2**, 1285 (1984).
[34] G. M. Turner, I. S. Falconer, B. W. James, and D. R. McKenzie, J. Appl. Phys. **65**, 3671 (1989).
[35] R. E. Muenchausen, K. M. Hubbard, S. Foltyn, R. C. Estler, N. S. Nogar, and C. Jenkins, Appl. Phys. Lett. **56**, 578 (1990).